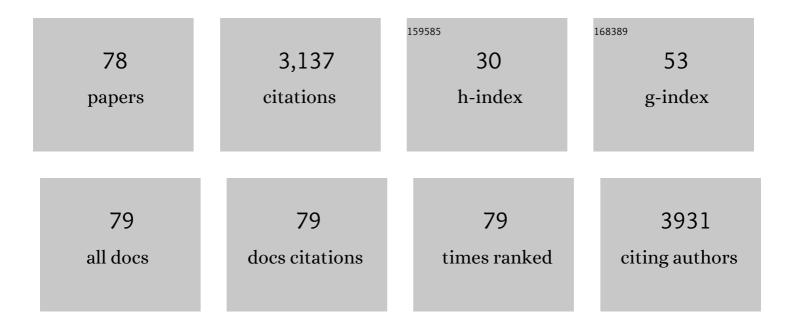
Qiao-Hong Li

List of Publications by Year in descending order

Source: https://exaly.com/author-pdf/2053301/publications.pdf Version: 2024-02-01



Οιλο-Ηονίς Γι

#	Article	IF	CITATIONS
1	TM3 (TMÂ=ÂV, Fe, Mo, W) single-cluster catalyst confined on porous BN for electrocatalytic nitrogen reduction. Journal of Materials Science and Technology, 2022, 108, 46-53.	10.7	19
2	Aluminum molecular rings bearing amino-polyalcohol for iodine capture. Inorganic Chemistry Frontiers, 2022, 9, 592-598.	6.0	9
3	Tunable third-order nonlinear optical effect <i>via</i> modifying Ti ₄ (embonate) ₆ cage-based ionic pairs. Inorganic Chemistry Frontiers, 2022, 9, 1984-1991.	6.0	8
4	Adsorption Behavior of Environmental Gas Molecules on Pristine and Defective MoSi ₂ N ₄ : Possible Application as Highly Sensitive and Reusable Gas Sensors. ACS Omega, 2022, 7, 8706-8716.	3.5	20
5	High-Throughput computational screening of Single-atom embedded in defective BN nanotube for electrocatalytic nitrogen fixation. Applied Surface Science, 2022, 591, 153130.	6.1	13
6	Black Titanium-Oxo Clusters with Ultralow Band Gaps and Enhanced Nonlinear Optical Performance. Journal of the American Chemical Society, 2022, 144, 8153-8161.	13.7	39
7	Silverâ€Templated γâ€Keggin Alkyltinâ€Oxo Cluster: Electronic Structure and Optical Limiting Effect. Angewandte Chemie - International Edition, 2022, 61, .	13.8	14
8	Silverâ€Templated γâ€Keggin Alkyltinâ€Oxo Cluster: Electronic Structure and Optical Limiting Effect. Angewandte Chemie, 2022, 134, .	2.0	1
9	Design of Hybrid Zeolitic Imidazolate Frameworkâ€Derived Material with C–Mo–S Triatomic Coordination for Electrochemical Oxygen Reduction. Small, 2021, 17, e2003256.	10.0	14
10	Combining a Titanium–Organic Cage and a Hydrogenâ€Bonded Organic Cage for Highly Effective Thirdâ€Order Nonlinear Optics. Angewandte Chemie, 2021, 133, 2956-2959.	2.0	9
11	Designable Al ₃₂ â€Oxo Clusters with Hydrotalciteâ€like Structures: Snapshots of Boundary Hydrolysis and Optical Limiting. Angewandte Chemie - International Edition, 2021, 60, 4849-4854.	13.8	39
12	Designable Al ₃₂ â€Oxo Clusters with Hydrotalciteâ€like Structures: Snapshots of Boundary Hydrolysis and Optical Limiting. Angewandte Chemie, 2021, 133, 4899-4904.	2.0	3
13	Combining a Titanium–Organic Cage and a Hydrogenâ€Bonded Organic Cage for Highly Effective Thirdâ€Order Nonlinear Optics. Angewandte Chemie - International Edition, 2021, 60, 2920-2923.	13.8	59
14	Defective Fe ₃ GeTe ₂ monolayer as a promising electrocatalyst for spontaneous nitrogen reduction reaction. Journal of Materials Chemistry A, 2021, 9, 6945-6954.	10.3	18
15	Functional ligand directed assembly and electronic structure of Sn ₁₈ -oxo wheel nanoclusters. Chemical Communications, 2021, 57, 5159-5162.	4.1	4
16	The exceptionally high moisture responsiveness of a new conductive-coordination-polymer based chemiresistive sensor. CrystEngComm, 2021, 23, 3549-3556.	2.6	7
17	Aluminium nanorings: configuration deformation and structural transformation. Chemical Communications, 2021, 57, 2085-2088.	4.1	10
18	Experimental and Theoretical Studies on Effects of Structural Modification of Tin Nanoclusters for Third-Order Nonlinear Optical Properties. Inorganic Chemistry, 2021, 60, 1885-1892.	4.0	21

QIAO-HONG LI

#	Article	IF	CITATIONS
19	Vertically Aligned MoS ₂ with In-Plane Selectively Cleaved Mo–S Bond for Hydrogen Production. Nano Letters, 2021, 21, 1848-1855.	9.1	63
20	Hybrid Zeolitic Imidazolate Frameworks for Promoting Electrocatalytic Oxygen Evolution via a Dual-Site Relay Mechanism. Inorganic Chemistry, 2021, 60, 3074-3081.	4.0	17
21	High-throughput screening of transition metal single-atom catalyst anchored on Janus MoSSe basal plane for hydrogen evolution reaction. International Journal of Hydrogen Energy, 2021, 46, 10337-10345.	7.1	30
22	MOF Nanosheet Reconstructed Twoâ€Dimensional Bionic Nanochannel for Protonic Fieldâ€Effect Transistors. Angewandte Chemie, 2021, 133, 10019-10023.	2.0	6
23	MOF Nanosheet Reconstructed Twoâ€Dimensional Bionic Nanochannel for Protonic Fieldâ€Effect Transistors. Angewandte Chemie - International Edition, 2021, 60, 9931-9935.	13.8	51
24	Theoretical screening of group IIIA-VIIA elements doping to promote hydrogen evolution of MoS2 basal plane. Applied Surface Science, 2021, 542, 148535.	6.1	31
25	Tin Metal Cluster Compounds as New Third-Order Nonlinear Optical Materials by Computational Study. Journal of Physical Chemistry Letters, 2021, 12, 7537-7544.	4.6	13
26	Interpenetrated Metal-Porphyrinic Framework for Enhanced Nonlinear Optical Limiting. Journal of the American Chemical Society, 2021, 143, 17162-17169.	13.7	85
27	Enhancing the hydrogen evolution reaction by non-precious transition metal (Non-metal) atom doping in defective MoSi2N4 monolayer. Applied Surface Science, 2021, 563, 150388.	6.1	49
28	Oriented Assembly of 2D Metal-Pyridylporphyrinic Framework Films for Giant Nonlinear Optical Limiting. Nano Letters, 2021, 21, 10012-10018.	9.1	28
29	Novel Third-Order Nonlinear Optical Materials with Craig-Möbius Aromaticity. Journal of Physical Chemistry Letters, 2021, 12, 11784-11789.	4.6	13
30	Theoretical screening of efficient single-atom catalysts for nitrogen fixation based on a defective BN monolayer. Nanoscale, 2020, 12, 1541-1550.	5.6	95
31	Three-in-One: Opened Charge-transfer channel, positively shifted oxidation potential, and enhanced visible light response of g-C3N4 photocatalyst through K and S Co-doping. International Journal of Hydrogen Energy, 2020, 45, 4534-4544.	7.1	46
32	High-performance of nanostructured Ni/CeO2 catalyst on CO2 methanation. Applied Catalysis B: Environmental, 2020, 268, 118474.	20.2	226
33	Heterometallic Ag ₂ Ti ₁₀ and Ag ₄ Ti ₈ -oxo clusters with different silver doping models: synthesis, structure, and theoretical studies. Dalton Transactions, 2020, 49, 11005-11009.	3.3	7
34	Accelerated design of photovoltaic Ruddlesden–Popper perovskite Ca6Sn4S14â^' <i>x</i> O <i>x</i> using machine learning. APL Materials, 2020, 8, .	5.1	9
35	N-Heterocyclic Carbene as a Surface Platform for Assembly of Homochiral Metal–Organic Framework Thin Films in Chiral Sensing. ACS Applied Materials & Interfaces, 2020, 12, 38357-38364.	8.0	20
36	Enhancing hydrogen evolution of MoS2 basal planes by combining single-boron catalyst and compressive strain. Frontiers of Physics, 2020, 15, 1.	5.0	20

QIAO-HONG LI

#	Article	IF	CITATIONS
37	Adsorption behavior of CO, CO2, H2, H2O, NO, and O2 on pristine and defective 2D monolayer ferromagnetic Fe3GeTe2. Applied Surface Science, 2020, 527, 146894.	6.1	20
38	2D Boron Imidazolate Framework Nanosheets with Electrocatalytic Applications for Oxygen Evolution and Carbon Dioxide Reduction Reaction. Small, 2020, 16, e1907669.	10.0	20
39	Atomically Precise Titanium–Oxo Nanotube with Selective Water Adsorption and Semiconductive Behaviors. CCS Chemistry, 2020, 2, 209-215.	7.8	14
40	Stable lead-free Te-based double perovskites with tunable band gaps: a first-principles study. New Journal of Chemistry, 2019, 43, 14892-14897.	2.8	32
41	A surface-mounted MOF thin film with oriented nanosheet arrays for enhancing the oxygen evolution reaction. Journal of Materials Chemistry A, 2019, 7, 18519-18528.	10.3	92
42	First-Principles Modeling of Lead-Free Perovskites for Photovoltaic Applications. Journal of Physical Chemistry C, 2019, 123, 3795-3800.	3.1	18
43	Pressure-induced effects in the inorganic halide perovskite CsGel ₃ . RSC Advances, 2019, 9, 3279-3284.	3.6	73
44	Photovoltaic Performance of Lead-Less Hybrid Perovskites from Theoretical Study. Journal of Physical Chemistry C, 2019, 123, 12638-12646.	3.1	39
45	Ethylammonium as an alternative cation for efficient perovskite solar cells from first-principles calculations. RSC Advances, 2019, 9, 7356-7361.	3.6	33
46	Atomic iridium@cobalt nanosheets for dinuclear tandem water oxidation. Journal of Materials Chemistry A, 2019, 7, 8376-8383.	10.3	72
47	Conductive metal–organic framework nanowire arrays for electrocatalytic oxygen evolution. Journal of Materials Chemistry A, 2019, 7, 10431-10438.	10.3	115
48	Theoretical Study of the Reverse Water Gas Shift Reaction on Copper Modified β-Mo ₂ C(001) Surfaces. Journal of Physical Chemistry C, 2019, 123, 1235-1251.	3.1	39
49	Predicted photovoltaic performance of lead-based hybrid perovskites under the influence of a mixed-cation approach: theoretical insights. Journal of Materials Chemistry C, 2019, 7, 371-379.	5.5	32
50	Metalâ€Free Fluorineâ€Đoped Carbon Electrocatalyst for CO ₂ Reduction Outcompeting Hydrogen Evolution. Angewandte Chemie - International Edition, 2018, 57, 9640-9644.	13.8	228
51	Metalâ€Free Fluorineâ€Doped Carbon Electrocatalyst for CO ₂ Reduction Outcompeting Hydrogen Evolution. Angewandte Chemie, 2018, 130, 9788-9792.	2.0	69
52	One-step synthesis of nonstoichiometric TiO ₂ nanorod films for enhanced photocatalytic H ₂ evolution. Dalton Transactions, 2018, 47, 4478-4485.	3.3	8
53	Incorporating Trialkylsilylethynyl-Substituted Head-to-Head Bithiophene Unit into Copolymers for Efficient Non-Fullerene Organic Solar Cells. ACS Applied Materials & Interfaces, 2018, 10, 7271-7280.	8.0	9
54	Cobalt Boron Imidazolate Framework Derived Cobalt Nanoparticles Encapsulated in B/N Codoped Nanocarbon as Efficient Bifunctional Electrocatalysts for Overall Water Splitting. Advanced Functional Materials, 2018, 28, 1801136.	14.9	155

QIAO-HONG LI

#	Article	IF	CITATIONS
55	Synergistic Effect of Doping and Compositing on Photocatalytic Efficiency: A Case Study of La ₂ Ti ₂ O ₇ . ACS Applied Materials & Interfaces, 2018, 10, 39327-39335.	8.0	17
56	Tailoring nonlinear optical crystal borophosphate through the introduction of transition metal d orbitals for improving optical anisotropy and SHG response: a first-principles investigation. Materials Research Express, 2018, 5, 096204.	1.6	0
57	CO ₂ Overall Splitting by a Bifunctional Metalâ€Free Electrocatalyst. Angewandte Chemie - International Edition, 2018, 57, 13135-13139.	13.8	64
58	CO 2 Overall Splitting by a Bifunctional Metalâ€Free Electrocatalyst. Angewandte Chemie, 2018, 130, 13319-13323.	2.0	15
59	Recent progress in improving the stability of copper-based catalysts for hydrogenation of carbon–oxygen bonds. Catalysis Science and Technology, 2018, 8, 3428-3449.	4.1	89
60	Innenrücktitelbild: Metal-Free Fluorine-Doped Carbon Electrocatalyst for CO2 Reduction Outcompeting Hydrogen Evolution (Angew. Chem. 31/2018). Angewandte Chemie, 2018, 130, 10133-10133.	2.0	0
61	Screening novel candidates for mid-IR nonlinear optical materials from I ₃ –V–VI ₄ compounds. Journal of Materials Chemistry C, 2017, 5, 1963-1972.	5.5	32
62	A comprehensive understanding of water photooxidation on Ag ₃ PO ₄ surfaces. RSC Advances, 2017, 7, 23994-24003.	3.6	13
63	Computation-predicted, stable, and inexpensive single-atom nanocatalyst Pt@Mo ₂ C – an important advanced material for H ₂ production. Journal of Materials Chemistry A, 2017, 5, 14658-14672.	10.3	34
64	Anatase TiO2 film composed of nanorods with predominantÂ{110} active facets as an excellent photocatalyst for water splitting. International Journal of Hydrogen Energy, 2017, 42, 5478-5484.	7.1	13
65	Inert Can Be Advantageous: Advisable Reconstruction and Application of Palladium Chloride for the Preferential Oxidation of the Hydrogen Impurity in Carbon Monoxide Streams. ChemCatChem, 2016, 8, 1909-1914.	3.7	10
66	An effective strategy to achieve deeper coherent light for LiB ₃ O ₅ . Journal of Materials Chemistry C, 2016, 4, 1926-1934.	5.5	24
67	Insights into the reaction mechanism of CO oxidative coupling to dimethyl oxalate over palladium: a combined DFT and IR study. Physical Chemistry Chemical Physics, 2015, 17, 9126-9134.	2.8	33
68	A novel Pd3O9@α-Al2O3 catalyst under a hydroxylated effect: high activity in the CO oxidation reaction. Physical Chemistry Chemical Physics, 2015, 17, 32140-32148.	2.8	5
69	Electrochemical preparation of metal–organic framework films for fast detection of nitro explosives. Journal of Materials Chemistry A, 2014, 2, 19473-19478.	10.3	111
70	Highly chemical and thermally stable luminescent Eu _x Tb _{1â^`x} MOF materials for broad-range pH and temperature sensors. Journal of Materials Chemistry C, 2014, 2, 8065-8070.	5.5	163
71	Strain-induced improvements on linear and nonlinear optical properties of SrB4O7 crystal. AIP Advances, 2012, 2, 032170.	1.3	15
72	Mechanism Insights into Second-Order Nonlinear Optical Responses of Anionic Metal Clusters. Journal of Cluster Science, 2011, 22, 365-380.	3.3	4

#	Article	IF	CITATIONS
73	Modulating the electronic structures and optical absorption spectra of BeO nanotubes by uniaxial strain. Applied Physics Letters, 2010, 97, 051901.	3.3	9
74	Magnetic properties of nonmetal atoms absorbed MoS2 monolayers. Applied Physics Letters, 2010, 96, .	3.3	199
75	Second-order nonlinear optical properties of transition metal clusters [MoS4Cu4X2Py2] (M = Mo, W;) Tj ETQq1 1	. 0.784314 2.8	ł rgBT /Over
76	Two cobalt(II) coordination polymers [Co2(H2O)4(Hbidc)2]n and [Co(Hbidc)]n (Hbidc =) Tj ETQq0 0 0 rgBT /Ove CrystEngComm, 2009, 11, 1054.	rlock 10 Tf 2.6	50 627 Td 53
77	Direct Metalâ	2.5	20
78	Solvent and Intermolecular Effects on First Hyperpolarizabilities of Organometallic Tungstenâ^'Carbonyl Complexes, A TDDFT Study. Journal of Physical Chemistry A, 2007, 111, 7925-7932.	2.5	19